UvA-DARE (Digital Academic Repository)

Built for the kill. Studies on the neutrophil NADPH oxidase

van Bruggen, R.

Publication date
2004

[Link to publication](#)

Citation for published version (APA):
van Bruggen, R. (2004). *Built for the kill. Studies on the neutrophil NADPH oxidase*.

Generation of mutations on potential FAD- binding residues in flavocytochrome b558 by a novel site-directed mutagenesis approach.

Robin van Bruggen[1,2], Christof Meischl[1] , Eloise Anthony[1], Michel Eppink[3], Willem van Berkel[3], Martin de Boer[1], Ron S. Weening[2] and Dirk Roos[1].

1 Sanquin Research, and Landsteiner Laboratory, Academic Medical Center, University of Amsterdam, Amsterdam, The Netherlands.

2 Emma Children's Hospital, Academic Medical Center, University of Amsterdam, Amsterdam, The Netherlands.

3Department of Biochemistry, Agricultural University, Wageningen, The Netherlands.

Introduction

The NADPH oxidase of phagocytes is the first identified and most extensively studied member of a family of enzymes involved in the generation of reactive oxygen species (ROS), collectively termed Noxes[1]. The phagocyte NADPH oxidase converts molecular oxygen to superoxide, in a reaction that uses NADPH as electron donor[2]. The superoxide formed by the phagocyte NADPH oxidase performs a defensive role; it is used by phagocytes to kill ingested microorganisms, after conversion into more aggressive reagents, such as HOCl and N-chloramines. In addition, potassium ion influx into the phagosome induced by the phagocyte NADPH oxidase is instrumental in the liberation of serine proteases from the proteoglycan matrix of the azurophil granules that have fused with the phagosome[3]. In contrast, the ROS generated by related Noxes appear to be involved in phenomena as diverse as cell growth, protein maturation, cross-linking of extracellular matrix proteins and defense against intracellular pathogens[1]. Although these enzymes appear to have differential functions, structurally they are highly homologous[1].

The phagocyte NADPH oxidase is an enzyme complex consisting of at least five proteins[4]. Two of them, gp91^{phox} and p22^{phox} form flavocytochrome b_{558}, the enzymatic core of the phagocyte NADPH oxidase. The other three essential proteins of the phagocyte NADPH oxidase, p47^{phox}, p67^{phox} and a small GTPase, Rac2, are necessary for the activation of the flavocytochrome[5]. Moreover, p67^{phox} and Rac2 have an important role in regulating the electron flow from NADPH to molecular oxygen[6;7].

Several groups have tried to elucidate structural characteristics of flavocytochrome b_{558}, leading to the identification of gp91^{phox} as the bearer of the electron transport chain needed for the generation of superoxide[8]. Gp91^{phox}, also known as Nox2, harbors two heme groups[9], one FAD molecule[10] and has an NADPH binding site[11]. The binding sites for the heme groups were previously identified by analysing the heme-binding capacity of gp91^{phox} mutants found in patients or in gp91^{phox} mutants generated by site-directed mutagenesis[12]. The requirement of histidine residues for binding of heme groups has greatly facilitated the identification of the exact binding sites for these redox groups[12]. A more challenging task is the identification of residues that bind FAD and NADPH. The residues in an FAD- or NADPH-binding fingerprint that directly bind to their ligand are less well defined than the histidines in heme binding. Few patient mutations are known that are located in putative FAD- or NADPH-binding

fingerprints[13;14]. Furthermore, most mutations in gp91[phox] identified in patients give rise to a truncated protein or completely abolish protein expression, leaving few informative mutants[15]. Therefore, the identification of FAD- and NADPH-binding residues by mutagenesis requires a large number of mutations, since the probability that the introduction of a mutation will lead to expression of a mutant with characteristics that will help to elucidate these binding sites is limited.

The generation of a large number of mutations on several residues in a protein is laborious and expensive. Numerous primers and PCR reactions are needed to introduce the mutations. Here, protein modelling and an efficient method to mutate residues were combined in an attempt to identify amino acids of gp91[phox] involved in FAD binding. First, two models of the cytoplasmic tail of gp91[phox] were generated, which were used to identify potential FAD-binding residues. Thereafter, a novel method was used to introduce different mutations on these amino-acid residues in one single reaction, a far more efficient method than existing site-directed mutagenesis protocols. The newly generated mutants were then expressed in cell lines and subsequently analysed for expression and function.

Materials and Methods

Purification of neutrophils and culture of cell lines.

Neutrophils were purified from heparinized blood as described[16] by centrifugation over isotonic Percoll, aspiration of plasma and mononuclear leukocytes, and lysis of RBCs with isotonic ammonium chloride. K562, PLB-985 and ϕnx-α cells were cultured in IMDM (Gibco) supplemented with 10% fetal calf serum, penicillin (200 μg/ml), streptomycin (200 μg/ml) and L-glutamine (4 mM) in a CO_2 incubator at 37°C.

Alignment of the cytoplasmic region of gp91[phox] with ferredoxin reductase and nitrate reductase, and construction of models.

The C-terminal part of gp91[phox] (amino acids 278-570) were aligned with the amino-acid sequences of ferredoxin reductase (1fdr) and nitrate reductase (1ndh) by means of Clustal. The C-terminus of gp91[phox] was then modelled on the crystal structures of 1fnb and 1ndh with the use of Insight II (MSI) on a Silicon Graphics Indigo.

Site-directed random mutagenesis.

Site-directed random mutagenesis was performed with the Quickchange mutagenesis kit (Stratagene), with degenerated primers designed according to the manufacturer's protocol. Mutagenesis was performed on cDNA of gp91^{phox} cloned into the pIRESpuro2 vector (Invitrogen). 75 colonies of each individual reaction were picked, and colony PCR was performed. Subsequently, 64 clones were sequenced by means of the Big Dye Terminator kit (Perkin Elmer). Samples were analysed on an ABI 377 automatic sequencer.

Transient expression of mutant gp91 in K562 cells.

K562 cells stably expressing p47^{phox} and p67^{phox} were transiently transfected with mutant gp91^{phox} by electroporation (0.25 kV, capacitance 960 μF, o Ω resistance), on a BioRad Biopulser. Cells were grown for 48 hours before analysis. Gp91^{phox} expression was assayed by flow cytometry. For this purpose, K562 cells were incubated with anti-gp91 MoAb 7D5 (kind gift from Dr. Michio Nakamura, Nagasaki, Japan) and then with goat-anti-mouse-Ig conjugated with phycoerythrin (Dako). K562 cells were analyzed on a Becton Dickinson FacsStar. H$_2$O$_2$ production of the transfected cells after phorbol myristate acetate (PMA, Sigma) activation was measured by the Amplex Red Assay (Molecular Probes) measured on a Perkin Elmer platereader.

Stable expression of selected mutants in PLB-985 cells.

PLB-985 X-CGD cells (a kind gift of Dr. M. Dinauer, Indianapolis, IN, USA) were retrovirally transduced with mutant gp91^{phox}. In brief, cDNA constructs encoding mutant gp91^{phox} were cloned from the pIRESpuro2 vector into the retroviral expression vector pLZRS. pLZRS constructs were then transfected into a retroviral packaging cell line (φnx-α) by calcium-phosphate transfection (Gibco). After selection of transfected cells with puromycin (1 μg/ml) (Gibco), virus was harvested and used for retroviral transduction of PLB-985 X-CGD cells with 10 μg/ml of Dotap (Roche). Transduced cells were stained with 7D5 and sorted on a FacsStar (Becton Dickinson) cell sorter.

Purification of flavocytochrome b_{558}.

Flavocytochrome b_{558} was purified by the method described by Cross et al[14]. In brief, plasma membranes of PLB-985 X-CGD cells expressing mutant gp91, or

plasma membranes from neutrophils isolated from healthy controls, were harvested as previously described[17]. The membranes were washed once with phosphate-buffered saline containing 1 M NaCl. After centrifugation (30 min 4°C 100,000g) the membranes were solubilized in 120 mM sodium-phosphate buffer pH 7.4, 1 mM EGTA, 1 mM dithiothreitol, 20% glycerol, 40 mM octyl-β-D-thioglucopyranoside (buffer A). The suspension was homogenized with a glass potter and subsequently stirred at 4°C. After a 1hr incubation in buffer A, insoluble material was pelleted by centrifugation (30 min, 100,000g). The supernatant was collected and submitted to absorption on a mixed-bed resin agarose (1/10 volume of the sample) consisting of equal volumes of CM sepharose, DEAE sepharose and ω-aminooctyl sepharose (all from Sigma). The unabsorbed material was then incubated with 1/10 vol of heparin agarose (Sigma) for one hour at 4°C, and washed batch-wise 3 times with 5 column volumes of buffer A. Flavocytochrome b_{558} was eluted with 1 volume of buffer A containing 0.6 M NaCl, and the eluate was diluted immediately with 2 volumes of buffer A.

Relipidation of purified flavocytochrome b_{558}.

The purified flavocytochrome was then relipidated by either one of the following procedures. (a) Dialysis: a portion of the diluted eluate was supplemented with phosphatidylcholine type IIs (Sigma) dissolved in buffer A by brief mixing on a Vortex, resulting in a final concentration of phosphatidylcholine of 100-200 µg/ml. This mixture was dialyzed for 18 h at 4°C against 200 volumes of buffer A lacking detergent. (b) Dilution: a portion of the diluted eluate was supplemented with phosphatidylcholine type IIs (Sigma) dissolved in buffer A to result in a final concentration of 400-500 µg/ml, and the final concentration of octyl-β-D-thioglucopyranoside was adjusted to 40 mM. It was then diluted with buffer A without detergent, to reduce the concentration of octyl-β-D-thioglucopyranoside to 8 mM and that of the phosphatidylcholine to 80-100 µg/ml, and allowed to stand at 4°C for at least 30 min.

Spectrophotometric analysis.

Flavocytochrome b_{558} concentration was measured by the reduced-minus-oxidized difference spectra, obtained with sodium dithionite as reducing agent. An extinction coefficient of 10.3 mM^{-1} was used for flavocytochrome b_{558} at 558 nm.

Determination of FAD-binding properties of flavocytochrome b_{558}.

Relipidated flavocytochrome b_{558} was placed in Slide-A-Lyzer cassettes (Pierce) with a volume of 1 ml (compartment B) and a molecular weight cut-off of 10 kD. Samples were dialyzed overnight against 2 L of buffer containing a fixed concentration of FAD (compartment A). FAD concentrations of different compartments were then analyzed by spectrophotometry according to the method of Faeder and Siegel[18]. In brief, 250 µl aliquots of sample were mixed with 650 µl of buffer B and 100 µl of 30% trichloro-acetic acid. Emission spectra were measured at 450 nm excitation.

Results

Identification of FAD-binding sites and selection of target residues.

First, we tried to identify the most probable FAD-binding residues within the FAD-binding fingerprints of gp91[phox]. For this purpose the cytoplasmic C-terminus of gp91[phox] (amino acids 278-570) was aligned with the amino-acid sequences of ferredoxin reductase (spinach) and nitrate reductase (pig). Among enzymes that have been crystallized, these enzymes have the highest homology with gp91[phox] (appr. 23%) (Figure 1).

After aligning gp91[phox] with both enzymes, it appears that gp91[phox] also has three FAD-binding regions, based on the identification of three stretches of residues that show homology with the FAD-binding parts of 1fdr and 1ndh (Figure 1, boxes). Besides FAD fingerprints, gp91[phox] also showed homology with parts of these enzymes that bind NADPH (not shown). These regions of gp91[phox] show considerable higher homology to both ferredoxin reductase and nitrate reductase than the rest of the C-terminus. After aligning gp91[phox] to both proteins, two models of the gp91[phox] C-terminus, based on the crystal structures of ferredoxin reductase and nitrate reductase, were constructed. The amino acids involved in FAD binding in these models were then identified, by measuring the distance between FAD and gp91[phox] residues (Figure 2).

We measured the distance between FAD and surrounding amino acids of gp91[phox] in these models and identified amino acids within 3Å of FAD as FAD-binding (Table 1). The data from both models were combined, and two residues were selected for mutagenesis, i.e. amino acids 369 and 370. These residues were

```
                10        20        30        40           50        60
               288       298       308       318          328       338
gp91   -LYLCERLVRFWRSQQKVVITKVVTHPFKTIELQMKKKGFK----MEVGQYIFVKCPKV-SKLEWHPFT-
1fdr   -----ADWVTGKVTKVQNWT-----DALFSLTVHAP------VLPFTAGQFTKLGLEIDG--RVQRAYSY
1ndh   STPAITLEDPDIKYPLRLIDKEVVDHDTRRFRFALP--SPEHILGLPVGQHIYLSARID-GNLVIRPYTP
                70        80        90       100       110
               348       358       368       378       388
gp91   LTSAPE-EDFFSIHIRIV-GDWTEGLFNAC-GCDKQEFQDAWKLPK-IAVDGPFGTASED----------
1fdr   VNSPDNPDLEFYLVT-VPDGKLSPRLAALKPG---DEVGVV------SEAAGFF--VLDE----------
1ndh   VSSDDD-KGFVDLVIKVY-FKDTHPKFPAG-GKMSQ-YLESMKIGDTIEFRGPNGLLVYQGKGKFAIRPD
               120
               398
gp91   VFS------YE
1fdr   VPH------CE
1ndh   KKSSPVIKTVK
```

Figure 1. Identification of FAD fingerprints in gp91^{phox}.
The cytoplasmic C-terminus of gp91^{phox} was aligned with ferredoxin reductase (1fdr) and nitrate reductase (1ndh). This figure shows the part of gp91^{phox} involved in FAD binding, the boxes indicate residues of gp91^{phox} that align with residues in 1fdr and 1ndh that are directly involved in binding FAD.

selected because of their involvement in FAD binding in both models. Other residues also displayed this feature, but they have already been identified previously to be involved in FAD binding in neutrophils of patients (i.e. His338[13]).

Generation of novel mutations on FAD-binding residues.

To generate different mutations of residues 369 and 370, a novel approach was used, which we named site-directed random mutagenesis. With this method, a specific residue is mutated into every possible amino acid in one PCR reaction, leading to a mixture of all possible mutants of this residue. For this purpose primers were used that were degenerated on the triplet of the target amino acid and therefore able to give rise to all possible amino acids on this residue. After running the mutagenesis PCRs, 64 clones of each residue were sequenced and 11 new mutations on position 369 and 15 on position 370 were identified (Table 2 and 3). None of the sequenced clones showed any additional, unwanted, mutation
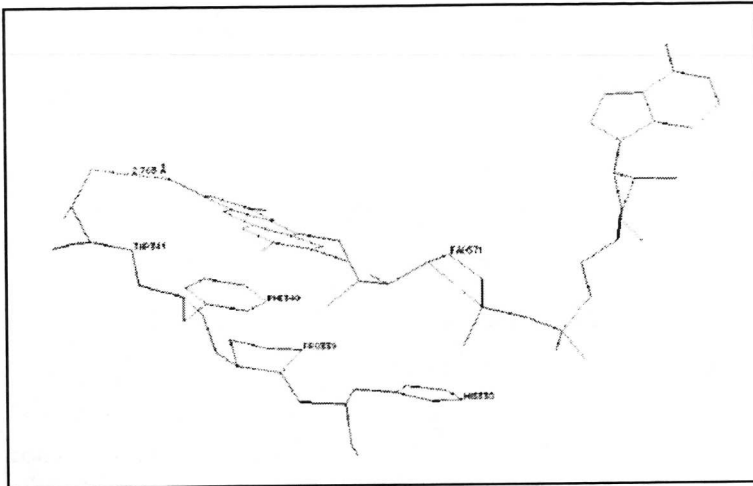
Figure 2. Measuring the distance between FAD and gp91^{phox} residues.
This figure shows a measurement of the distance between the cytoplasmic C-terminus of gp91^{phox} and FAD in one of the models (model based on homology with 1fdr). The distance between FAD and Thr 341 was measured, identifying Thr 341 as an FAD-binding residue in this model (distance is 2.73Å). This approach was used for all FAD surrounding amino acids in the two models, leading to the identification of the FAD-binding residues (Table 1).

Table 1. Residues identied as FAD-binding in models of gp91phox	
model based on 1fdr amino acid	model based on 1ndh amino acid
	Tyr324
His338	His338
Pro339	Pro339
Phe340	Phe340
Thr341	
Arg356	Arg356
Asp360	
	Trp361
Cys369	Cys369
Gly370	Gly370
Cys371	
	Asp372

Table 1. Residues identied as FAD-binding in models of gp91^{phox}.
Distance of residues in models of gp91^{phox} were measured with InsightII (Figure 2). Amino acids residues of gp91^{phox} within 3Å of FAD were defined as FAD-binding. Data from both models were combined to select amino acids for mutagenesis.

clone	mutation	expression	H2O2
12	C369C	pos	10000
26	C369STOP	neg	0
10	C369F	pos	7000
22	C369I	pos	0
7	C369L	pos	2000
52	C369N	pos	0
57	C369M	pos	9000
23	C369Q	pos	7000
16	C369R	pos	0
29	C369S	pos	3000
14	C369T	pos	9000
2	C369V	pos	3500

Table 2. Mutations generated on position 369.

clone	mutation	expression	H2O2
7	G370G	pos	10000
36	G370STOP	neg	0
3	G370A	pos	9000
9	G370C	pos	8000
22	G370E	pos	3000
60	G370F	pos	10000
15	G370I	pos	0
8	G370K	pos	10000
37	G370L	pos	6000
54	G370N	pos	14000
24	G370P	pos	0
43	G370Q	pos	11000
49	G370R	pos	3000
20	G370S	pos	6500
26	G370T	pos	2000
10	G370V	pos	2500

Table 3. Mutations generated on position 370.

Table 2 and 3. Mutations generated on position 369 and 370.

Expression and hydrogen-peroxide-producing capacity of site-directed random mutants on position 369. The number of cells tested for hydrogen peroxide production was corrected for the percentage of $gp91^{phox}$-positive cells in each individual transfection. Values are given as relative fluorescence units (RFUs), with wild-type $gp91^{phox}$-transfected cells at 10,000 RFUs The RFUs generated by untransfected cells were subtracted. A representative experiment from three experiments is shown.

Expression and analysis of new mutants in K562 cells.

The newly generated $gp91^{phox}$ mutants were transiently expressed in K562 cells that already stably express $p47^{phox}$ and $p67^{phox}$, by electroporation. After transfection with wild-type $gp91^{phox}$, these cells are able to produce superoxide when stimulated with PMA (not shown). Expression of mutant $gp91^{phox}$ on the plasma membrane of transfected cells was determined by flow cytometric analysis with mAb 7D5. All new mutants of $gp91^{phox}$ were expressed, except the mutants bearing a stop codon at the targeted amino acid residue (Table 2 and 3). We then assayed the superoxide-producing capacity of the $gp91^{phox}$ mutants indirectly by measuring the amount of hydrogen peroxide produced after PMA stimulation. As expected, K562 cells transfected with wild-type $gp91^{phox}$ generated hydrogen peroxide, whereas untransfected cells or cells transfected with a mutant $gp91^{phox}$ bearing a stop codon did not generate hydrogen peroxide after PMA stimulation (Table 2 and 3). For both residues, several mutations that completely abolished hydrogen peroxide production as well as mutations that seemed to diminish the hydrogen peroxide production were identified (Table 2 and 3). Two G370 mutants seemed to enhance this capacity (Table 3).

FAD-binding capacity of mutant gp91[phox].

To determine the effects of the new mutations on FAD binding, flavocytochrome b_{558} was isolated from the membranes of retrovirally transduced PLB-985 X-CGD cells. In general, approximately 600 pmol of flavocytochrome b_{558} was obtained per mutant, determined by spectrophotometry (Figure 3). To set up the FAD-binding assay, flavocytochrome b_{558} was isolated from normal human neutrophils and relipidated. FAD binding was then assayed by equilibrium dialysis and subsequent measurement of the FAD concentration in the two compartments by spectrophotometry. However, binding of FAD to flavocytochrome b_{558}, at different concentrations of this protein, was not observed (Table 4). Apo-D-amino acid oxidase (a-AAO) was used as a control in this system, and this enzyme showed FAD binding (Table 4). To ensure that the two subunits of flavocytochrome b_{558} were intact after overnight dialysis the reduced-minus-oxidized difference spectrum was measured (Figure 3) and a Western blot was performed to detect
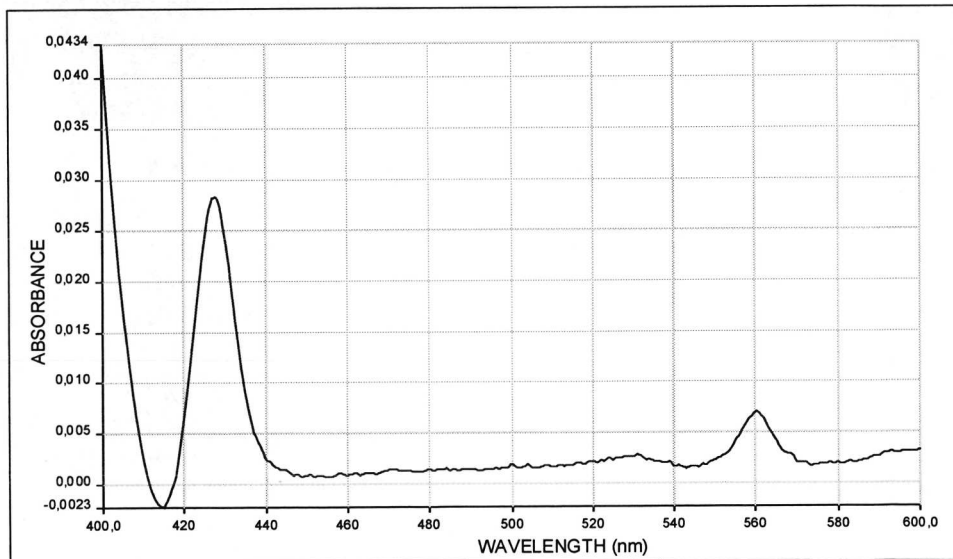

Figure 3. Reduced-minus-oxidized difference spectrum of flavocytochrome b_{558}.
Flavocytochrome b_{558} samples were purified from membranes of human neutrophils. The dithionite-reduced-minus-oxidized difference spectra were analyzed as described in Materials and Methods. The result shown is representative for purified flavocytochrome b_{558} obtained by our purification protocol.

Table 4. FAD binding capacity of purified cytochrome b558.

Sample in compartment B	[FAD] Compartment A	[FAD] Compartment B
Buffer	198.6+/-3.2 nM	201.4+/-4.3 nM
100 nM cytochrome b558	199.5+/-4.1 nM	196.2+/-2.7 nM
200 nM cytochrome b558	202.8+/-3.8 nM	206.2+/-2.5 nM
100 nM a-AAO	200.4+/-3.7 nM	280.3+/-2.9 nM
200 nM a-AAO	195.1+/-4.6 nM	364.3+/-3.0 nM

Table 4. FAD-binding capacity of purified flavocytochrome b_{558}.
The FAD-binding capacity of purified flavocytochrome b_{558} was assayed by equilibrium dialysis. Samples (compartment B) were dialyzed overnight against 2000 volumes of buffer containing 200 nM FAD (compartment A). As a positive control for FAD binding apo-D-amino acid oxidase (a-AAO) was taken. Buffer alone was used as negative control. Valuesare the mean of three individual experiments.

breakdown of gp91^{phox} and/or p22^{phox} (Figure 4). The spectra of the overnight dialyzed sample showed no differences with the spectra of the sample at the start of the procedure. Furthermore, Western blotting revealed identical staining patterns of both subunits before and after dialysis, excluding the possibility of truncation of the proteins and subsequent loss of FAD binding during dialysis. Several attempts were then made to improve the FAD binding of flavocytochrome b_{558} by adjusting the relipidation of the enzyme. Two different relipidation protocols were tried, one based on dialysis, the other based on dilution of the sample. Both strategies led to lowering of the concentration of detergent and to subsequent incorporation of flavocytochrome b_{558} into liposomes, resulting in the restoration of FAD binding by flavocytochrome b_{558}. However, none of the tested protocols provided flavocytochrome b_{558} that was able to bind FAD.

Discussion

In this report we combined protein modelling and a simple method to mutate a particular amino acid into any other amino acid to identify FAD-binding residues in flavocytochrome b_{558}. This strategy was used to generate informative mutants in a simple and efficient way.

The identification of residues that were likely to be involved in FAD binding was achieved by using the information provided by two models of the cytoplasmic tail of gp91^{phox}. Two residues were selected that were within 3Å of FAD in both models, a cysteine at position 369 and a glycine at position 370. Mutagenesis of these residues was performed by a novel approach, based on the
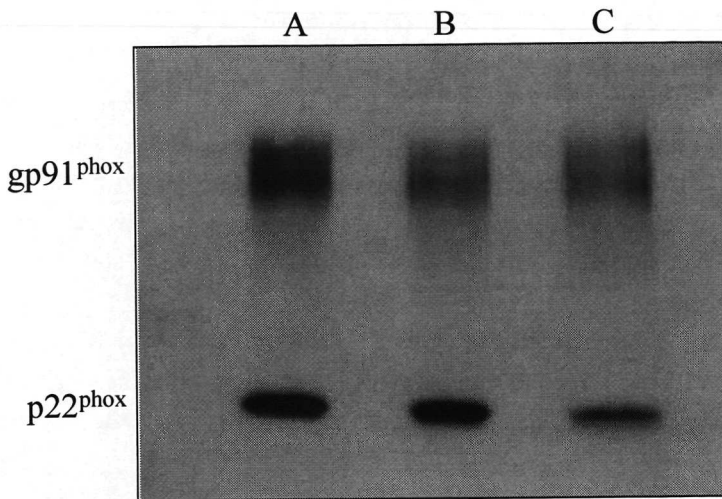
Figure 4. Western Blot analysis of subunits of purified cytochrome b_{558}.
Proteolytic degradation of gp91[phox] and p22[phox] was determined by Western blot. Both subunits were tested for changes in molecular weight after overnight dialysis. Pre- (A) and Post-dialysis (B) samples were compared with a total cell lysate of neutrophils (C) for differences in gp91[phox] and p22[phox] chain length.

use of degenerated primers, which allows the generation of any mutation on the selected residue. A high number of new mutants was generated, which were all expressed on the plasma membrane of K562 cells. This was a surprising finding, because mutations in gp91 are infamous for disturbing expression of flavocytochrome b_{558}[19]. This might argue against the use of K562 cells for this kind of studies, since one could reason that gp91[phox] expression in this system is not comparable with primary neutrophils. However, we have expressed several patient mutations in these cells and discrepancies in expression levels of the different gp91[phox] mutants between neutrophils and our K562 model were never observed.

Attempts were then made to measure the FAD binding capacity of the different mutants. Unfortunately, FAD binding to wild-type flavocytochrome b_{558}, isolated from human neutrophils could not be measured, indicating that our purification/relipidation protocol was malfunctioning. Spectrophotometric analysis and Western blotting indicated that the isolated flavocytochrome b_{558} was intact, suggesting that the relipidation of the flavocytochrome, which is essential for FAD binding, was unsuccessful. A lot of effort was put into optimising the relipidation protocol, but no apparent increase was observed in the FAD-binding capacity of the isolated flavocytochrome. To determine the effects of the new mutations,

several other approaches were tried. The cytoplasmic part of gp91^{phox}, tagged N-terminally with 6 histidines for purification, was expressed in several different expression systems, including baby hamster kidney cells (BHK), *Pichia pastoris* and *Escherichia coli*. Only expression in *E.coli* led to a high production of His-tagged gp91^{phox} C-terminus, but this fusion protein was expressed in inclusion bodies. Isolation of the fusion protein from these inclusion bodies was successful, but the subsequent refolding of the protein to a soluble, FAD-binding state was not achieved (data not shown).

Although new mutations in a putative FAD-binding region of gp91^{phox} were generated, the effect of these mutations on FAD-binding capacity of gp91^{phox} has still to be determined before any conclusions can be drawn on the structural effects of these mutations.

Reference List

1. Lambeth JD. Nox/Duox family of nicotinamide adenine dinucleotide (phosphate) oxidases. Curr Opin Hematol. 2002;9:11-17.

2. Roberts J, Camacho Z. Oxidation of NADPH by polymorphonuclear leucocytes during phagocytosis. Nature. 1967;216:606-607.

3. Reeves EP, Lu H, Jacobs HL, et al. Killing activity of neutrophils is mediated through activation of proteases by K+ flux. Nature. 2002;416:291-297.

4. Bokoch GM, Diebold BA. Current molecular models for NADPH oxidase regulation by Rac GTPase. Blood. 2002;100:2692-2696.

5. Vignais PV. The superoxide-generating NADPH oxidase: structural aspects and activation mechanism. Cell Mol Life Sci. 2002;59:1428-1459.

6. Nisimoto Y, Motalebi S, Han CH, Lambeth JD. The p67(phox) activation domain regulates electron flow from NADPH to flavin in flavocytochrome b(558). J Biol Chem. 1999;274:22999-23005.

7. Diebold BA, Bokoch GM. Molecular basis for Rac2 regulation of phagocyte NADPH oxidase. Nat Immunol. 2001;2:211-215.

8. Babior BM. The respiratory burst oxidase. Hematol Oncol Clin North Am. 1988;2:201-212.

9. Yu L, Quinn MT, Cross AR, Dinauer MC. Gp91(phox) is the heme binding subunit of the superoxide-generating NADPH oxidase. Proc Natl Acad Sci U S A. 1998;95:7993-7998.

10. Light DR, Walsh C, O'Callaghan AM, Goetzl EJ, Tauber AI. Characteristics of the cofactor requirements for the superoxide-generating NADPH oxidase of human polymorphonuclear leukocytes. Biochemistry. 1981;20:1468-1476.

11. Doussiere J, Brandolin G, Derrien V, Vignais PV. Critical assessment of the presence of an NADPH binding site on neutrophil cytochrome b558 by photoaffinity and immunochemical labeling. Biochemistry. 1993;32:8880-8887.

12. Biberstine-Kinkade KJ, DeLeo FR, Epstein RI, LeRoy BA, Nauseef WM, Dinauer MC. Heme-ligating histidines in flavocytochrome b(558): identification of specific histidines in gp91(phox). J Biol Chem. 2001;276:31105-31112.

13. Yoshida LS, Saruta F, Yoshikawa K, Tatsuzawa O, Tsunawaki S. Mutation at histidine 338 of gp91(phox) depletes FAD and affects expression of cytochrome b558 of the human NADPH oxidase. J Biol Chem. 1998;273:27879-27886.

14. Yu L, Cross AR, Zhen L, Dinauer MC. Functional analysis of NADPH oxidase in granulocytic cells expressing a delta488-497 gp91(phox) deletion mutant. Blood. 1999;94:2497-2504.

15. Roos D, de Boer M, Kuribayashi F, et al. Mutations in the X-linked and autosomal recessive forms of chronic granulomatous disease. Blood. 1996;87:1663-1681.

16. Weening RS, Schoorel EP, Roos D, et al. Effect of ascorbate on abnormal neutrophil, platelet and lymphocytic function in a patient with the Chediak-Higashi syndrome. Blood. 1981;57:856-865.

17. Leusen JH, Meischl C, Eppink MH, et al. Four novel mutations in the gene encoding gp91-phox of human NADPH oxidase: consequences for oxidase assembly. Blood. 2000;95:666-673.

18. Faeder EJ, Siegel LM. A rapid micromethod for determination of FMN and FAD in mixtures. Anal Biochem. 1973;53:332-336.

19. Roos D, de Boer M, Kuribayashi F, et al. Mutations in the X-linked and autosomal recessive forms of chronic granulomatous disease. Blood. 1996;87:1663-1681.